Penerbit Akademia Baru

Journal of Advanced Research in Materials Science
ISSN (online): 2289-7992 | Vol. 10, No.1. Pages 26-39, 2015

The Effect of Polyethylene-grafted-Maleic Anhydride as Compatibilizer on Properties of Recycled High Density Polyethylene/Ethylene Vinyl Acetate/Taro Powder (*Colocasia esculenta*) Composites

A.R.H. Fatimah[*1,a], *A.G. Supri*[2,b], *and Z. Firuz*[1,c]

[1]School of Materials Engineering, Universiti Malaysia Perlis (UniMAP), Kompleks Taman Muhibah, Jejawi 2, 02600 Arau, Perlis, Malaysia.
[2]Faculty of Engineering Technology, Universiti Malaysia Perlis (UniMAP), Main Campus, Pauh Putra, 02600 Arau, Perlis, Malaysia.
[a,*]*fatimahrajak@gmail.com*, [b]*supri@unimap.edu.my*, [c]*firuz@unimap.edu.my*

Abstract - *The objectives of this study were to investigate the effects of filler loading and compatibilizer, namely taro powder (TP) and polyethylene-grafted-maleic anhydride (PE-g-MAH) on the tensile properties, swelling behavior, water absorption, morphology analysis, infrared spectroscopy, and thermal stability of recycled high density polyethylene (RHDPE)/ ethylene vinyl acetate (EVA)/ taro powder (TP) composites. In this regard, RHDPE/EVA/TP composites were prepared by using melt blending technique in a Brabender Plasticorder at temperature of 160°C and speed of 50 rpm. The results showed the tensile strength and elongation at break decreased with increasing TP loading while modulus of elasticity, mass swell, water absorption, and thermal stability increased. Nevertheless, the addition of PE-g-MAH greatly improved the tensile strength, modulus of elasticity, and thermal stability. However, the elongation at break, percentage mass swell, and water absorption decreased with the corporation of PE-g-MAH as compatibilizer. The scanning electron microscopy (SEM) results revealed that taro powder filler dispersed in RHDPE/EVA/TP phase composites and better dispersion state of dispersed taro was discovered in RHDPE/EVA/TP composites with addition of PE-g-MAH as compatibilizer. On the other hand, adding PE-g-MAH also resulted in better interfacial adhesion between RHDPE/EVA matrix and TP filler.*

Keywords: Polymer Composites, Natural Filler, Compatibilizer, Taro Powder, Polyethylene-grafted-Maleic Anhydride

1.0 INTRODUCTION

Composites are an essential group of materials for many engineering applications as they form an important part in many areas such as marine, aircraft, and automotive industries [1]. Composites can be described as materials that comprise of two or more chemically and

Journal of Advanced Research in Materials Science
ISSN (online): 2289-7992 | Vol. 10, No.1. Pages 26-39, 2015

physically different phases divided by a distinct interface which having bulk properties considerably dissimilar from those of any of the constituents. The different materials combined together to achieve a composite with required mechanical strength and stiffness [2].

The addition of fillers into polymer matrix has become the fastest and cheapest way to alter the properties of the base polymer. In recent years, natural fibers have been extensively used as reinforcing fillers in thermoplastic-polymer composite materials [3]. Natural fillers can be applied as replacement for conventional synthetic fibers like glass fibers due to their low density, low price, problem-free disposal, good thermal insulation, and good mechanical properties [4]. Taro (*Colocasia esculenta*) is herbaceous plants which grow in fast speed and cause problem to occur such as thick vegetation. This thick vegetation happened to be the breeding grounds for mosquitoes, poisonous creatures, and other diseases course [5]. The high content of starch in taro, 25-30%, is the most valid reason it can be used in industry because this feature gives the ease of digestibility of taro. Taro can be applied as fillers or modifiers for plastics when their starch is used in the production of plastic which can help to accelerate the biodegradability of the parent polymer [6]. Nevertheless, the main drawback of natural fillers is the lack of good interfacial adhesion between the two components because of the hydrophilic nature of the natural filler which is not compatible to the hydrophobic polymer matrix [7].

The interface properties of the polymeric composites can be promoted to better interfacial adhesion through the usage of compatibilizers. The compatibilizers have the ability to react with both natural fillers and the polymers by providing paths or building bridges across the interface [8]. Majid et al. [9] had studied the effect of PE-g-MAH on tensile properties and morphology of low density polyethylene/ thermoplastic sago starch-kenaf fiber. As a results, the tensile strength and Young's modulus of LDPE/TPSS-kenaf fiber composites with the addition of PE-g-MAH were greater than the composites without the addition of PE-g-MAH particularly at high fiber loading.

The objectives of this study are to fabricate recycled high density polyethylene/ ethylene vinyl acetate/ taro powder composites and to investigate taro powder suitability as potential filler polymer composites. Moreover, the effect of polyethylene-grafted-maleic anhydride as compatibilizer on processibility, tensile properties, swelling behavior, water absorption, morphology, infrared spectroscopy, and thermal stability were systematically investigated.

2.0 EXPERIMENTAL

2.1 Materials

Recycled high density polyethylene (RHDPE) and ethylene vinyl acetate (EVA) were used as the matrix of the composites in this work. The RHDPE has a melt flow index of 0.7 g/10min at 190°C and a density of 0.9399 g/cm^3 while the EVA, contains 18.1wt% vinyl acetate (VA), with melt flow index of 2.5 g/10min at 80°C and a density of 0.926-0.950 g/cm^3 were used. Both of the materials were supplied by A. R. Alatan Sdn. Bhd., Kedah Darul Aman, Malaysia. Taro powder (TP) filler was obtained from local village in Selangor, Malaysia. The ingredients of TP were shown in Table 1. Polyethylene-grafted-maleic anhydride containing 0.85wt% of maleic anhydride and dibenzoyl peroxide (DBP) with 75% of water were also obtained from A.R. Alatan Sdn. Bhd., Kedah Darul Aman, Malaysia.

Table 1: Ingredients of taro powder filler was tested from Laboratory Department of DXN Holdings Bhd., Jitra, Kedah.

Content	Quantity
Calories (Kcal)	274
Carbohydrate (%)	52.6
Fat (%)	1.2
Protein (%)	13.1

2.2 Composite Preparation

For the TP preparation, the stems from taro plants was cut, washed, dried, and grinded to powder by using grinder machine. The TP filler will be sieved to average size of 75 µm and dried back in a vacuum oven at 80°C for one hour before used for composite processing. For the composites preparation, the compounding of the composites was carried out by melt blending technique using Brabender Plasticoder internal mixer. The RHDPE was first mixed in the internal mixer at temperature of 160°C and speed of 50rpm for 2 min, followed by addition of EVA and both materials will be mixed until homogenous. The compatibilizer, PE-g-MAH, dibenzoyl peroxide (DBP), and TP were added to the internal mixer for the remaining minutes. After that, the softened RHDPE/EVA/TP and RHDPE/EVA/TP/PE-g-MAH composites were removed from the chamber and pressed into thick, round pieces of compounding. Table 2 shows the formulations used in this study.

Table 2: Formulation of RHDPE/EVA/TP and RHDPE/EVA/TP/PE-g-MAH composites.

Composite Code	RHDPE [phr]	EVA [phr]	TP [phr]	PE-g-MAH [phr]	DBP [phr]
RHDPE/EVA/TP5	80	20	5	-	-
RHDPE/EVA/TP10	80	20	10	-	-
RHDPE/EVA/TP15	80	20	15	-	-
RHDPE/EVA/TP20	80	20	20	-	-
RHDPE/EVA/TP25	80	20	25	-	-
RHDPE/EVA/TP5/PE-g-MAH	80	20	5	6	1
RHDPE/EVA/TP10/PE-g-MAH	80	20	10	6	1
RHDPE/EVA/TP15/PE-g-MAH	80	20	15	6	1
RHDPE/EVA/TP20/PE-g-MAH	80	20	20	6	1
RHDPE/EVA/TP25/PE-g-MAH	80	20	25	6	1

2.3 Compression Molding

In order to produce the composites in plate form, the hydraulic hot press was used. The machine was set at temperature of 160°C both at top and bottom platen. Empty mold was heated for 5 minutes before used. Then composites were put into the mold, preheated and compressed partially for 8 minutes. Once the composites started to soften, they were fully compressed for 6 minutes. After compression, the composites were allowed to cool for another 4 minutes.

2.4 Tensile Test

Tensile properties were determined according to ASTM D-638 by using the Universal Testing Machine Instron 5569 with crosshead speed of 30mm/min. Dumbbell shaped specimens were conditioned at ambient temperature (25±3)°C and relative humidity (30±2)% before the testing.

An average of ten samples was used for each formulation. The tensile strength, elongation at break, and Young's modulus of each formulation were obtained from the test.

2.5 Swelling Behavior Test

The swelling behavior test was carried out in general accordance with ISO 1817. Samples with dimension of 20mm x 10mm x 2mm were used for each composites composition. The samples were totally immersed into test tubes containing dichloromethane for 46 hours. After immersion period, the samples were removed from dichloromethane and blotted with tissue paper before weighed by using an analytical balance with 0.1 mg resolution. The degree of swelling (weight increase) was calculated as follows:

$$(\%)\text{Mass Swell} = \frac{(W_s - W_o) \times 100}{W_o} \quad (1)$$

Where W_o is the initial weight of sample; W_s is the weight of the swollen sample after immersion.

2.6 Water Absorption Test

The composite specimens used to determine water absorption behaviour were immersed in distilled water at room temperature in accordance to ASTM D570. The amount of water absorbed was measured every 24 hours for 3 days and every 1 week for two months. At regular intervals, the specimens were taken out from the water and wiped with filter paper to remove surface water and weighed with digital scale. The samples were re-immersed in water to permit the continuation of sorption. The weighing was done within 30s, in order to avoid error. The percentage of apparent weight gain was then calculated according to equation:

$$Water\ absorption\ (\%) = \frac{W_a - W_b x 100}{W_b} \quad (2)$$

Where W_b is the initial weight of sample; W_a is the weight of the swollen sample after immersion.

2.7 Scanning Electron Microscopy

The morphology of the fracture surfaces of blends were studied by using scanning electron microscope model JEOL JSM-6460LA. Before the examination of SEM, the samples were mounted on aluminium stubs and allowed to undergo sputtering coating. A thin platinum layer of 20nm was sputter coated on the samples surfaces to avoid electrostatic charged during examination.

2.8 Fourier Transform Infrared (FTIR) Spectroscopy

The FTIR spectra were obtained by using Perkin-Elmer Spectrum 400 Series equipment. The selected spectrum resolution and the scanning range were 4cm^{-1} and 650-4000cm^{-1}, respectively. The FTIR spectra with % transmittance (%T) versus wavelength (cm^{-1}) were gained after scanning process.

2.9 Thermogravimetric Analysis (TGA)

Thermogravimetry analysis of the compositess was done by using Perkin-Elmer Pyris 6 TGA analyser. Samples of about 10mg were scanned from 50 to 650°C with a heating rate of 10°C/min by using constant nitrogen gas flow of 50ml/min to prevent thermal oxidation

Journal of Advanced Research in Materials Science
ISSN (online): 2289-7992 | Vol. 10, No.1. Pages 26-39, 2015

process of polymer sample. The temperature at 50% weight loss ($T_{-50\%wt}$), final decomposition temperature (FDT) and the residual mass of the thermogravimetric curves were calculated.

3.0 RESULTS AND DISCUSSION

3.1 Tensile Properties

Figure 1 presents the effect of filler loading and compatibilizer on tensile strength of RHDPE/EVA/TP and RHDPE/EVA/TP/PE-g-MAH composites. Both of composites progressively decreased in tensile strength with increasing of filler loading. This was due to the increased in filler content caused agglomeration of fillers particles, consequently reduced tensile strength of the composites. Quiroz-Castillo et al. [10] reported that tensile strength showed a decreasing trend with increased of chitosan content because of the brittleness of chitosan which reduced the ductility. Aderikha & Shapovalov [11] revealed that addition of micro-sized fillers introduced weak interfaces because of poor wetting and negligible adhesion which resulted in reducing tensile strength proportional to the filler content.

By comparing both graphs, with similar TP loading, RHDPE/EVA/TP/PE-g-MAH composites exhibited higher tensile strength than RHDPE/EVA/TP composites. This can be explained by the presence of PE-g-MAH which made easy transfer of the slight stress at interfacial adhesion between matrix and filler through the deformation. The accumulation of compatibilizer enhanced interfacial adhesion of the matrixes while providing interaction between anhydride groups of maleic anhydride to the hydroxyl groups of TP, thus improving matrix-filler interaction.

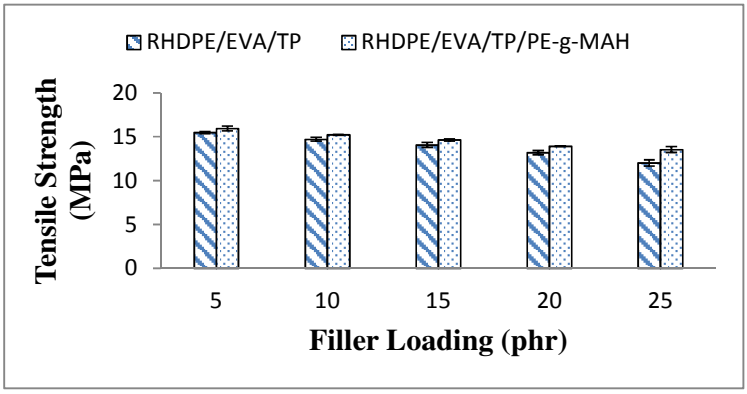

Figure 1: Effect of filler loading and compatibilizer on tensile strength of RHDPE/EVA/TP and RHDPE/EVA/TP/PE-g-MAH composites.

Figure 2 exhibits elongation at break of RHDPE/EVA/TP and RHDPE/EVA/TP/PE-g-MAH composites. The elongation at break of RHDPE/EVA/TP and RHDPE/EVA/TP/PE-g-MAH decreased as filler loading increased. This can be attributed to the restriction of elastic properties of the composites with reduction in matrix due to increase of TP filler. The deformation of TP is generally less than RHDPE/EVA matrix, therefore addition of filler forces matrix to deform more than the total deformation of composites.

From Figure 2, elongation at break for RHDPE/EVA/TP composites is higher than RHDPE/EVA/TP/PE-g-MAH composites. The results were explained by high stiffness of TP filler than matrix which can increase the tensile modulus but commonly cause a significant

Penerbit Akademia Baru
Journal of Advanced Research in Materials Science
ISSN (online): 2289-7992 | Vol. 10, No.1. Pages 26-39, 2015

reduction in elongation at break of composites. The decreasing trend of elongation at break for RHDPE/EVA/TP/PE-g-MAH was a recognizable signal of improved interfacial adhesion between RHDPE/EVA phases and TP filler after the addition of PE-g-MAH as compatibilizer.

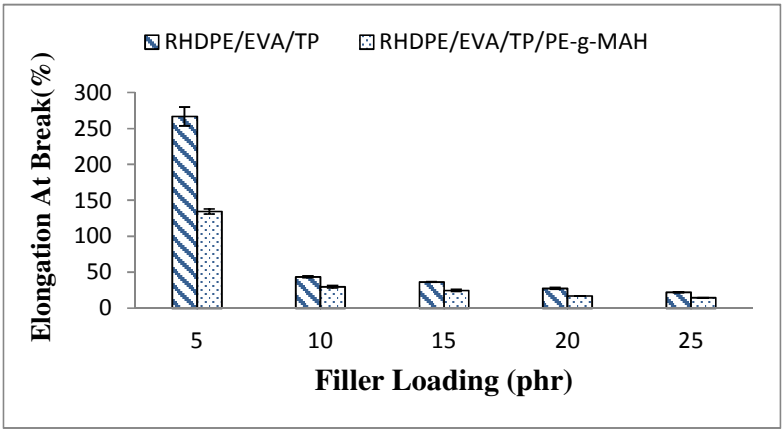

Figure 2: Effect of filler loading and compatibilizer on elongation at break of RHDPE/EVA/TP and RHDPE/EVA/TP/PE-g-MAH composites.

The effects of filler loading and compatibilizer on modulus of elasticity of RHDPE/EVA/TP and RHDPE/EVA/TP/PE-g-MAH composites were denoted in Figure 3. Both graphs of the composites revealed an increasing in modulus of elasticity in a manner proportional to the TP content. As TP is stiff in character, an increase in TP content result in a decrease in ductility of composites, hence increased tensile modulus. On the other hand, Adhikary et al. [12] reported that tensile modulus of HDPE/wood flour increased with increasing the fiber content due to the composite material became stiffer.

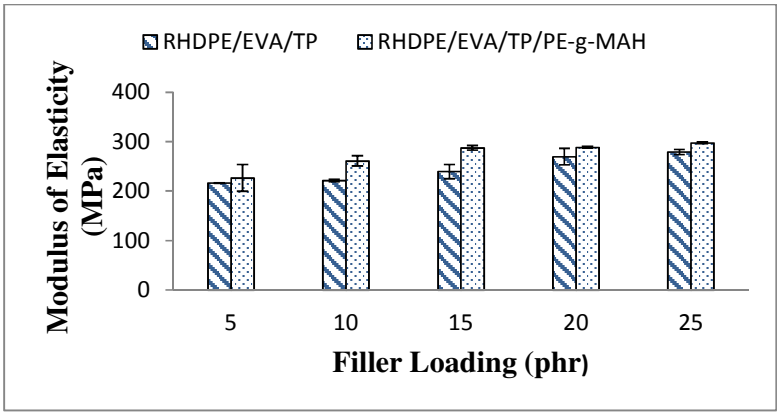

Figure 3: Effect of filler loading and compatibilizer on modulus of elasticity of RHDPE/EVA/TP and RHDPE/EVA/TP/PE-g-MAH composites.

As comparison between uncompatibilized and compatibilized composites, RHDPE/EVA/TP/PE-g-MAH composites displayed higher modulus of elasticity than RHDPE/EVA/TP composites at different filler loading. The addition of PE-g-MAH preferentially located at the interface between two polymers results in lowering interfacial tension, and improved the compatibility of TP and the matrix. Improvement in stiffness of

Journal of Advanced Research in Materials Science
ISSN (online): 2289-7992 | Vol. 10, No.1. Pages 26-39, 2015

composite effect the modulus of elasticity values of both composites. According to Ismail et al. [13], addition of white rice husk ash (WRHA) to NR/LLDPE blends will increase the tensile modulus and higher tensile modulus will be achieved by addition of poly-(propylene-ethylene-acrylic acid) (PPEAA) as compatibilizer which improved the filler-matrix bonding by efficient stress transfer from the matrix to the filler phases.

3.2 Swelling Behavior

Figure 4 shows the effect of filler loading and compatibilizer on percentage mass swell of RHDPE/EVA/TP and RHDPE/EVA/TP/PE-g-MAH composites. From Figure 4, percentage mass swell of both composites increased with increasing the TP content. This was due to the hydrophilicity of TP which absorbed more dichloromethane into the composites.

At similar filler loading, RHDPE/EVA/TP/PE-g-MAH composites show lower percentage of mass swell than RHDPE/EVA/TP composites. This was due to the chemical bonding of acrylic anhydride group of PE-g-MAH with polar group of TP filler and RHDPE/EVA matrix, where ester bonding and hydrogen bonding had already been formed, resulted in better interfacial adhesion. This had caused lower dichloromethane intake into the composites which reduced mass swell of RHDPE/EVA/TP/PE-g-MAH.

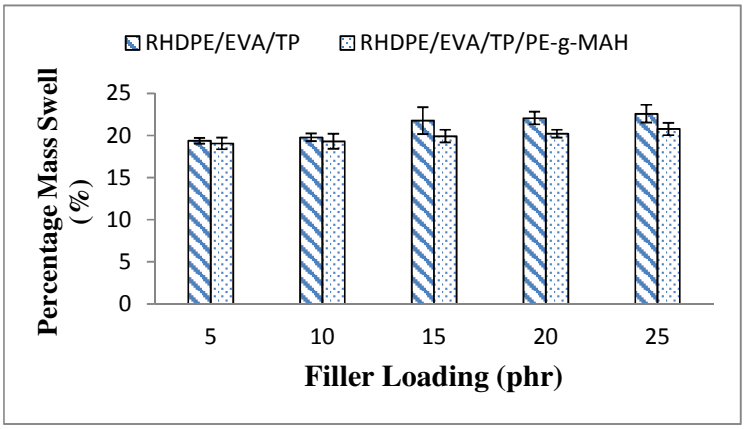

Figure 4: Effect of filler loading and compatibilizer on percentage mass swell of RHDPE/EVA/TP and RHDPE/EVA/TP/PE-g-MAH composites.

3.3 Water Absorption

Figure 5 demonstrates the effect of filler loading and presence of PE-g-MAH as compatibilizer on the water absorption of the RHDPE/EVA/TP composites. It was found that with higher percentage of TP filler loading, the TP fillers will form extended and contacting chains, which will enhances the penetration of water into RHDPE/EVA/TP composites. This will resulted in increased percentage of water intake of the overall material [14].

From Figure 5, the water absorption of RHDPE/EVA/TP composites is much higher than RHDPE/EVA/TP/PE-g-MAH composites. This was because of the presence of PE-g-MAH as compatibilizer which compatibilized the composites, thus reduced penetration of water into RHDPE/EVA/TP composites due to better dispersion of filler surrounded by core [15]. Ashori & Shesmani [16] observed the addition of maleated anhydride grafted polypropylene (MAPP) as coupling agent to composites of recycled polypropylene (RPP) with combination of recycled newspaper fiber (RNF) and poplar wood flour (PWF) as reinforcement. They concluded that

Penerbit Akademia Baru

Journal of Advanced Research in Materials Science
ISSN (online): 2289-7992 | Vol. 10, No.1. Pages 26-39, 2015

addition of MAPP to the composites exhibited lower water absorption by improving the quality of adhesion between polymer and fibers.

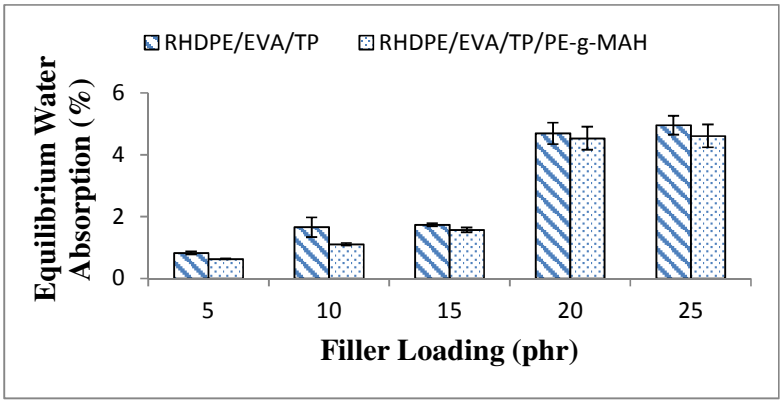

Figure 5: Effect of filler loading and compatibilizer on equilibrium water absorption of RHDPE/EVA/TP and RHDPE/EVA/TP/PE-g-MAH composites.

3.4 Morphology Analysis

The SEM micrographs of tensile fractured surface of RHDPE/EVA/TP and RHDPE/EVA/TP/PE-g-MAH composites at different filler loading were examined in Figure 6 (a-c). From Figure 7 (a-c), RHDPE/EVA/TP/PE-g-MAH composites show better filler dispersion compared to RHDPE/EVA/TP composites at similar filler loading in Figure 6. The micrographs clearly showed the strong bonding demonstrated from reduced number of holes around the RHDPE/EVA matrix and breaking of TP as filler. PE-g-MAH as a compatibilizer decreased the interfacial tension between matrix and filler, providing better dispersion of the filler in the matrix. Besides that, it can be observed that RHDPE/EVA/TP/PE-g-MAH composites presented rougher surface which indicated better interfacial adhesion between matrix and filler in comparison to RHDPE/EVA/TP.

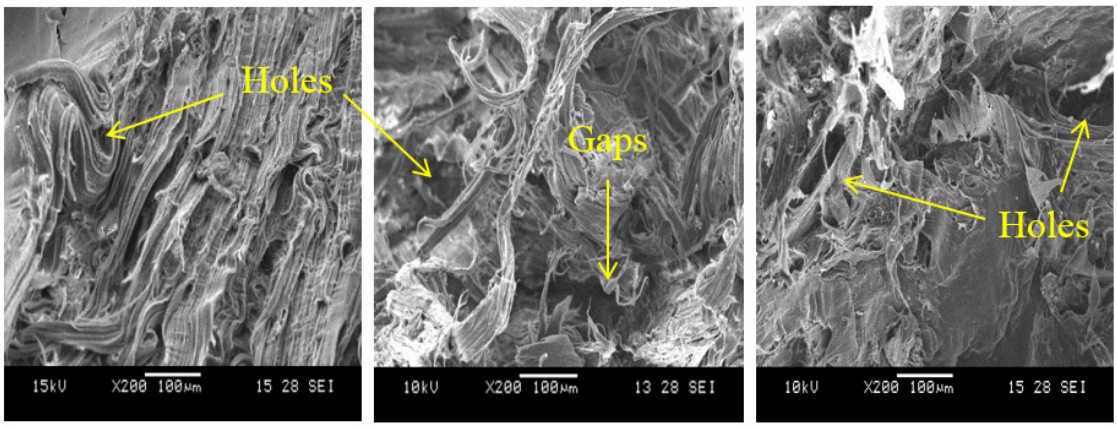

(a) RHDPE/EVA/TP-5 (b) RHDPE/EVA/TP-15 (c) RHDPE/EVA/TP-25

Figure 6: SEM micrograph of tensile fractured surface of RHDPE/EVA/TP composites.

Penerbit Akademia Baru

Journal of Advanced Research in Materials Science
ISSN (online): 2289-7992 | Vol. 10, No.1. Pages 26-39, 2015

3.5 Spectroscopy Infrared Analysis

The FTIR spectra for taro powder filler (TP) was examined in Figure 8 From the spectra shown, TP exhibited strong and broad stretch frequency at 3426.95 cm^{-1}, corresponding to strong presence of O-H in cellulose of TP. The band at 2919.76 cm^{-1} for TP can be attributed to strong C-H alkanes stretching while at frequency 1624.40 cm^{-1} represented the presence of C=C of aromatic ring based on TP frequency above 3000 cm^{-1}. Besides that, another sharp peak also displayed the band at 1384.16 cm^{-1} and 1320.14 cm^{-1}, conforming O-H bending in plane and deformation of CH_2 in TP. The C-O strong stretching vibration of the cellulose backbone disclosed at frequency of 1055.03 cm^{-1} which displayed with two peaks. The band at 780.93 cm^{-1} represents medium C-H out-of-plane bending and peak at 638.49 cm^{-1} presented the C-H deformation in taro powder.

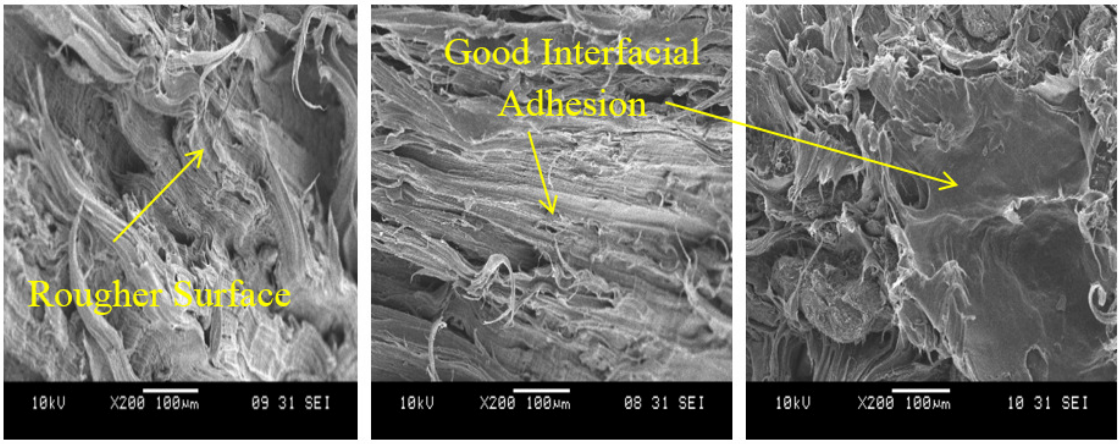

(a) RHDPE/EVA/TP-5/ PE-g-MAH

(b) RHDPE/EVA/TP-15/ PE-g-MAH

(c) RHDPE/EVA/TP-25/ PE-g-MAH

Figure 7: SEM micrograph of tensile fractured surface of RHDPE/EVA/TP composites.

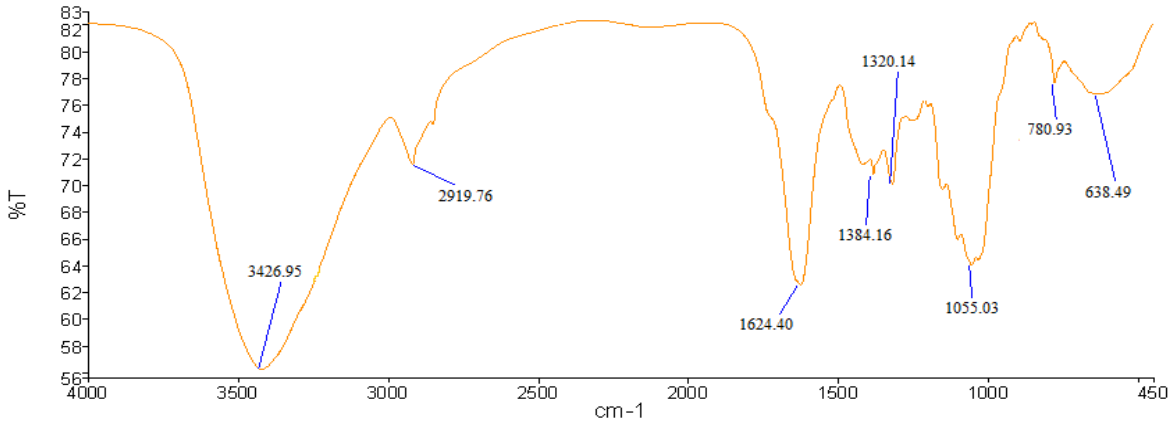

Figure 8: The FTIR spectrum of RHDPE/EVA/TP.

Figure 9 shows FTIR spectra of RHDPE/EVA/TP and RHDPE/EVA/TP/PE-g-MAH respectively. Both graphs exhibited strong C-H stretching in 2917.72 cm^{-1} and 2917.64 cm^{-1} attributed to methyl group from RHDPE with strong formation of C-H_2 and C-H at peaks of

Penerbit Akademia Baru
Journal of Advanced Research in Materials Science
ISSN (online): 2289-7992 | Vol. 10, No.1. Pages 26-39, 2015

2849.47 cm^{-1} and 2849.35 cm^{-1}. Besides that, RHDPE/EVA/TP/PE-g-MAH composites displayed more obvious band at 1738.59 cm^{-1} than RHDPE/EVA/TP at frequency 1739.9 cm^{-1}, related to ester group due to the carbonyl (C=O) group from aliphatic stretching group. The apparent peak in RHDPE/EVA/TP/PE-g-MAH also indicated presence of PE-g-MAH which showed chemical reaction of ester group from EVA with anhydride group (-CO-O-OC-) from PE-g-MAH. The absorption peak at frequency range 1370 cm^{-1} revealed the medium C-O bending in-plane cause by existence of TP, while O-C stretching ester group clearly represented by band at 1240 cm^{-1} with RHDPE/EVA/TP/PE-g-MAH presented two broad peaks due to formation of new bond between EVA and PE-g-MAH. Nevertheless, all bands in the range from 700 cm^{-1} to 900 cm^{-1} for both graphs were allocated to the strong C-H bending vibration.

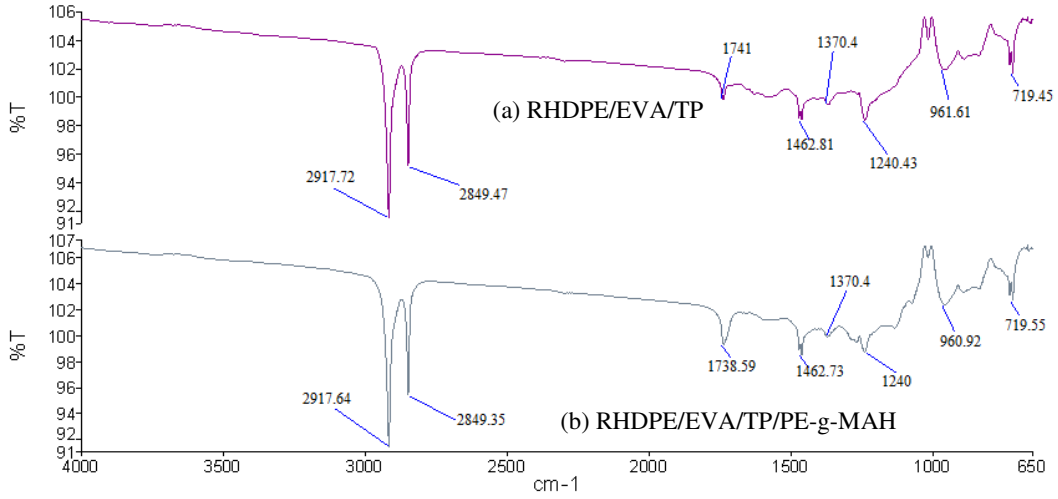

Figure 9: The FTIR spectra of (a) RHDPE/EVA/TP-15 and (b) RHDPE/EVA/TP-15/PE-g-MAH composites.

3.6 Thermal Degradation

Figure 10 and Figure 11 show the typical thermal degradation curves of RHDPE/EVA/TP and RHDPE/EVA/TP/PE-g-MAH composites with different filler loading. Table 3 shows that the temperature of 50% weight loss and residual mass for RHDPE/EVA/TP and RHDPE/EVA/TP/PE-g-MAH composites increased with the increasing of filler loading. This result indicated that higher filler loading gives the RHDPE/EVA/TP and RHDPE/EVA/TP/PE-g-MAH composites more thermal stability than composites with lower filler loading.

From Table 3, it can also be seen that temperature of 50% weight loss ($T_{-50\%wt}$) and residual mass of RHDPE/EVA/TP/PE-g-MAH composites are higher than RHDPE/EVA/TP composite. This was due to the presence of good interfacial adhesion between RHDPE/EVA and TP phase as a result of uniform dispersion of filler throughout RHDPE/EVA matrix. The better dispersion of filler acts as a barrier against the release of volatilization gases during thermal degradation. It may also attribute to an adsorption effect of these gases at filler surface which slowed down polymer degradation [17].

Penerbit Akademia Baru
Journal of Advanced Research in Materials Science
ISSN (online): 2289-7992 | Vol. 10, No.1. Pages 26-39, 2015

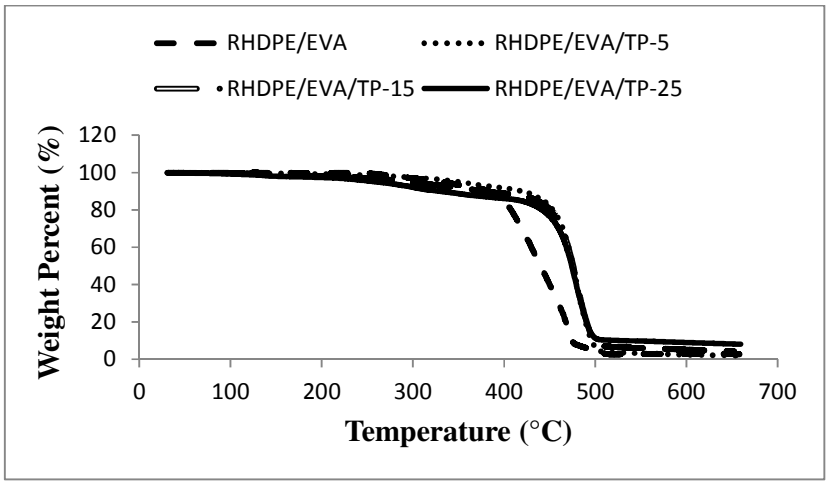

Figure 10: Thermogravimetric curves of RHDPE/EVA/TP composites at different filler loading.

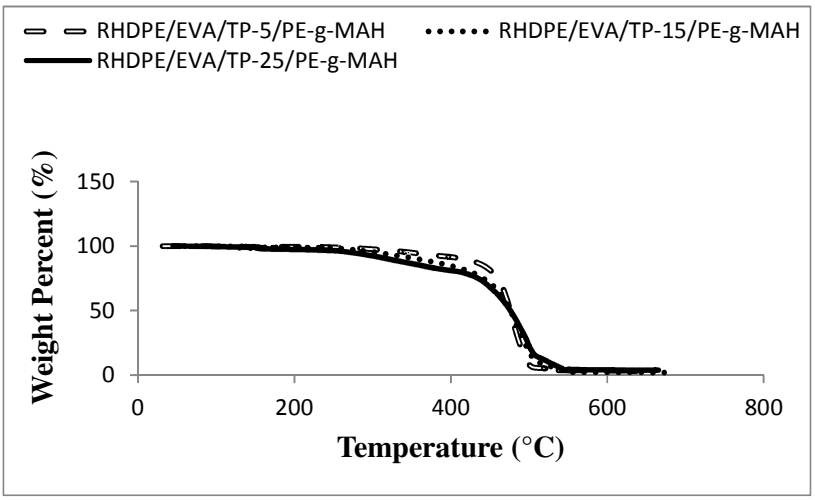

Figure 11: Thermogravimetric curves of RHDPE/EVA/TP/PE-g-MAH composites at different filler loading.

Table 3: Temperature of 50% weight loss ($T_{-50\%wt}$) and residual mass for RHDPE/EVA/TP and RHDPE/EVA/TP/PE-g-MAH composites.

Blend Composition	$T_{-50\%wt}$ (°C)	Residual Mass (%)	Decomposition Peak (°C)
RHDPE/EVA	440.12	2.051	467.25
RHDPE/EVA/TP-5	475.57	2.100	476.77
RHDPE/EVA/TP-15	475.82	4.299	477.81
RHDPE/EVA/TP-25	476.29	8.059	476.32
RHDPE/EVA/TP-5/PE-g-MAH	475.86	3.501	476.18
RHDPE/EVA/TP-15/PE-g-MAH	476.03	5.111	476.96
RHDPE/EVA/TP-25/PE-g-MAH	476.41	8.947	498.31

Penerbit Akademia Baru
Journal of Advanced Research in Materials Science
ISSN (online): 2289-7992 | Vol. 10, No.1. Pages 26-39, 2015

Figure 12 shows the derivative thermogravity (DTG) of RHDPE/EVA/TP composites with different TP filler loading. There are two degradation peaks (°C) of RHDPE/EVA composites without the presence of TP filler loading. The two endothermic peaks of RHDPE/EVA composites can be attributed to significant weight loss due to the EVA degradation (415-419 °C) and RHDPE decomposition (465-470 °C) respectively. This finding indicates that the composites decomposed at this temperature range which the decomposers volatilized and caused the weight loss while the decomposition absorbed heat [18]. However, the addition of TP makes the material more thermally stable by introducing only one thermal decomposition stage. A more simple result is shown in Figure 13 where the effects of PE-g-MAH are shown. The differential thermal curves show only one endothermic peak proves that the thermal decompositions of RHDPE/EVA/TP/PE-g-MAH were a single-step reaction and indicates the effectiveness of PE-g-MAH as compatibilizer. The differential thermal curves and peak temperatures of all the composites in Figure 12 and Figure 13 show the changes in thermal decomposition temperature with different filler loading and addition of compatibilizer. The decomposition temperature increased as TP filler increased followed the rule of thermal decomposition of organic compounds due to increase in covalent bond between matrix and filler.

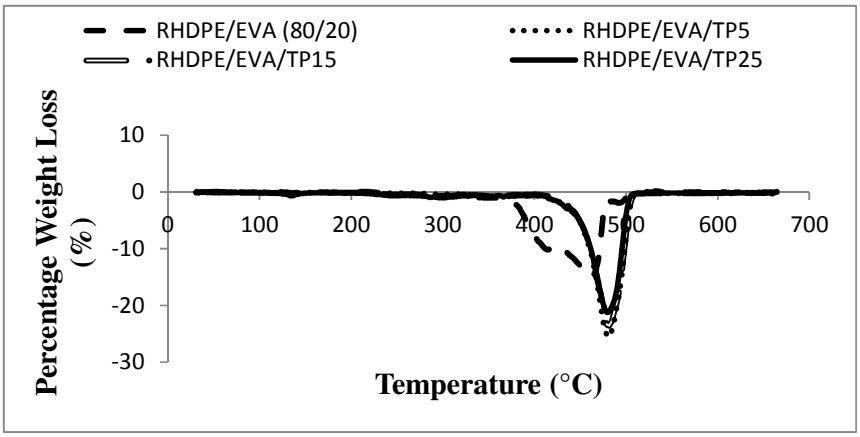

Figure 12: DTG thermogram of RHDPE/EVA/TP composites at different filler loading.

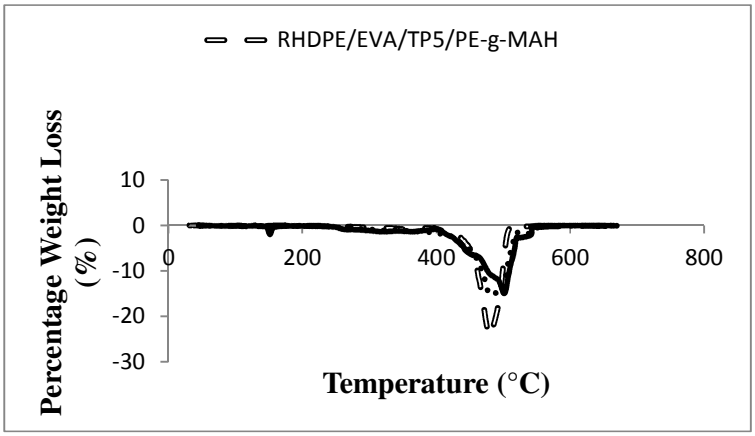

Figure 13: DTG thermogram of RHDPE/EVA/TP/PE-g-MAH composites at different filler loading.

4.0 CONCLUSIONS

The modulus of elasticity and thermal stability of the RHDPE/EVA/TP composites were noticeably improved by the addition of TP filler while tensile strength, elongation at break, swelling behavior, and water absorption decreased. The compatibilizer, PE-g-MAH was found to be effective in improving the tensile strength, modulus of elasticity, and thermal stability of RHDPE/EVA/TP/PE-g-MAH. The PE-g-MAH had more pronounced strength properties and modulus than the thermal properties. The swelling behavior and water absorption of the composites increased gradually with increasing TP filler loading. The SEM micrographs display better compatibility between matrix and filler in addition of PE-g-MAH. Based on the findings, the RHDPE/EVA/TP/PE-g-MAH composites can be used in applications requiring high strength and thermal stability.

REFERENCES

[1] A. Fotouh, J.D. Wolodko, M.G. Lipsett, Fatigue of natural fiber thermoplastic composites, Composites: Part B 62 (2014) 175-182.

[2] S. Jana, B. Laha, S. Maiti, Boswelia gum resin/chitosan polymer composites: Controlled delivery vehicles for aceclofenac, International Journal of Biological Macromolecules 77 (2015) 303-306.

[3] X. Luo, J. Li, J. Feng, S. Xie, X. Lin, Evaluation of distillers grains as fillers for low density polyethylene: Mechanical, rheological and thermal characterization, Composites Science and Technology 89 (2013) 175-179.

[4] N. Ayrilmis, A. Kaymakci, F. Ozdemir, Physical, mechanical, and thermal properties of polypropylene composites filled with walnut shell flour, Journal of Industrial and Engineering Chemistry 19 (2013) 908-914.

[5] T. Bindu, V.P. Sylas, M. Mahesh, P.S. Rakesh, E.V. Ramasamy, Pollutant removal from domestic wastewater with Taro (Colocasia esculenta) planted in a subsurface flow system, Ecological Engineering 33 (2008) 68-82.

[6] R.H. Howeler, C.G. Oates, G.M. O'Brien, Cassava, starch, and starch derivatives, Proceedings of the International Symposium, Guangxi, China, 1996.

[7] N. Bakar, C.Y. Chee, L.C. Abdullah, C.T. Ratnam, N. Azowa, Effect of methyl methacrylate grafted kenaf on mechanical properties of polyvinyl chloride/ethylene vinyl acetate composites, Composites: Part A 63 (2014) 45-50.

[8] B.I. Ugheoke, N.O. Namesan, R.M. Joshua, R.N. Ufodi, The effect of processing methods on some properties of rice husk-polypropylene composites, National Postgraduate Conference, Kuala Lumpur, 2011.

[9] R.A. Majid, H. Ismail, R.M. Taib, Effects of polyethylene-g-maleic anhydride on properties of low density polyethylene/thermoplastic sago starch reinforced kenaf fibre composites, Iran Polymer Journal 19 (2010) 501-510.

[10] J.M. Quiroz-Castillo, D.E. Rodriguez-Felix, H. Grijalva-Monteverde, T. del-Castillo Castro, M. Plascencia-Jatomea, F. Rodriguez-Felix, P.J. Herrera-Franco, Preparation of

Journal of Advanced Research in Materials Science
ISSN (online): 2289-7992 | Vol. 10, No.1. Pages 26-39, 2015

extruded polyethylene/chitosan blends compatibilized with polyethylene-graft-maleic anhydride, Carbohydrate Polymers 101 (2014) 1094-1100.

[11] V.N. Aderikha, V.A. Shapovalov, Mechanical and tribological behavior of PTFE polyoxadiazole fiber composites. Effect of filler treatment, Wear 271 (2011) 970-976.

[12] K.B. Adhikary, S. Pang, M.P. Staiger, Dimensional stability and mechanical behavior of wood-plastic composites based on recycled and virgin high-density polyethylene (HDPE), Composites: Part B Engineering 39 (2008) 807-815.

[13] H. Ismail, J.M. Nizam, H.P.S. Abdul Khalil, The effect of a compatibilizer on the mechanical properties and mass swell of white rice husk ash filled natural rubber/linear low density polyethylene blends, Polymer Testing 20 (2001) 125-133.

[14] S. Tamrakar, R.A. Lopez-Anido, Water absorption of wood polypropylene composite sheet piles and its influence on mechanical properties, Construction and Building Materials, 25 (2011) 3977-3988.

[15] H. Hong, H. Liao, H. Zhang, H. He, T. Liu, D. Jia, Significant improvement in performance of recycled polyethylene/wood flour composites by synergistic compatibilization at multi-scale interfaces, Composites: Part A 64 (2014) 90-98.

[16] A. Ashori, S. Sheshmani. Hybrid composites made from recycled materials: Moisture absorption and thickness swelling behavior, Bioresource Technology, 101 (2010) 4717-4720.

[17] A.G. Supri, H. Ismail, The effect of isophorone diisocyanate-polyhydroxyl groups modified water hyacinth fibers (Eichhornia crassiper) on properties of low density polyethylene/acrylonitrile butadiene styrene (LDPE/ABS) composites, Polymer Plastic Technology Engineering 50 (2011) 113-120.

[18] C. Yuan, B. Liu, H. Liu, Characterization of hydroxypropyl-β-cyclodextrins with different substitution patterns via FTIR, GC-MS, and TG-DTA, Carbohydrate Polymers 118 (2015) 36-40.